

Lineament and Depth Evaluation of Magnetic Sources in a Geological Transition Zone of Abeokuta and its environs, Southwestern Nigeria

Hazeez Owolabi Edunjobi ^{1*}, Gideon Oluyinka Layade ¹, Michael Oluwaseyi Falufosi ² and Oluwaseun Tolulope Olurin ¹

¹ Department of Physics, Federal University of Agriculture, Abeokuta, Nigeria

² Department of Geology, University of Ibadan, Nigeria

Received January 18, 2021; Accepted April 16, 2021

Abstract

The study location is Abeokuta and its environs situated on a geological transition zone Precambrian migmatic and Cretaceous sedimentary rock units of the Abeokuta group. Qualitative and quantitative analyses of a High Resolution Aeromagnetic (HRAM) data of Abeokuta and its environs (sheet 260) acquired from the Nigerian Geological Survey Agency (NGSA) were interpreted to determine the geologic structures the area is composed of, as well as the sedimentary thickness of the location. The qualitative analysis was achieved by reduction to the magnetic equator and lineaments extraction by applying different filters for enhancement of magnetic anomalies, while the quantitative analysis aided the estimation of depth to basement of magnetic sources by Source Parameter Imaging (SPI) and 3D Euler Deconvolution methods. The qualitative interpretation revealed the distribution of magnetically susceptible anomalies with areas of low, intermediate and high magnetic intensities distributed across the study area. The lineament extraction map showed clearly the possible fault zones majorly trending northeast of the study area. The depth weighting techniques revealed a depth to basement range of 145 to 903 m for the SPI and 102 to 985 m for 3D Euler Deconvolution. These depth ranges also show that the sedimentary cover is thicker at the south and southwestern zones of the study area, considered sufficient for the exploration of igneous, metamorphic and sedimentary rock minerals. Interpretation of structural features has also provided detailed information on the geology of the study area like discerning areas competent for engineering construction and possible mineral traps.

Keywords: Abeokuta; Dahomey Basin; Magnetic sources; Lineaments; Euler deconvolution.

1. Introduction

Aeromagnetic survey can be useful in the delineation of structural features like lineaments, folds, faults, dyke and sills. In general, a judgmental component of geological mapping and mineral resources intervention programmes in many nations is airborne geophysics [1]. The recent use of this survey method ensures the widest coverage of areas of interest, even if inaccessible. Over the years, aeromagnetic survey has proven reliable in the investigation of magnetic and non-magnetic anomalous sources within and around the basement complex and sedimentary terrains [2-3].

The desire to deepen the body of knowledge and characterize the subsurface features for better understanding of geology of the study area led to this research. This study is targeted at addressing geologically related challenges using High Resolution Aeromagnetic (HRAM) Data. For instance, with sedimentary thickness (depth to basement) evaluation, one can predict the rock or mineral potentials of an area of interest [4]. Also, the knowledge of fractured regions can help in siting engineering works like road construction and founding high-rise buildings. Groundwater development is another societal problem that can be solved through this method because the basement topography controls the accumulation and distribution of groundwater around the transition zone [5].

The study location is Abeokuta and its environs, a part of eastern Dahomey basin, southwestern Nigeria and number of researchers have worked in the study area using different methods of geophysical surveying; Layade *et al.* [6] used a Bouguer gravity dataset to extract source parameters defining the area by forward and inverse modelling technique [7]. also used rock petrography and geologic mapping to determine the various lithological features and rock types in the metropolis of Abeokuta. [8-10] used aeromagnetic method for the estimation of depth and source location of anomalies in the study location.

Other researchers have also used methods employed in this study; Thompson [11] used the Source Parameter Imaging (SPI™) method to compute the source parameters from gridded magnetic data. Okpoli *et al.* and Osinowo *et al.* [12-13] used 3D – Euler Deconvolution method to estimate the depth to aeromagnetic anomalous sources.

1.1. Description and geology of the study area

Dahomey Basin, otherwise referred to as the Benin Basin is an assemblage of inland, coastal and offshore basin that expands from southeastern Ghana to southwestern Nigeria through Togo and the Republic of Benin [14-15]. It is separated from the Niger Delta region of the country by a subsurface basement high called the Okitipupa ridge.

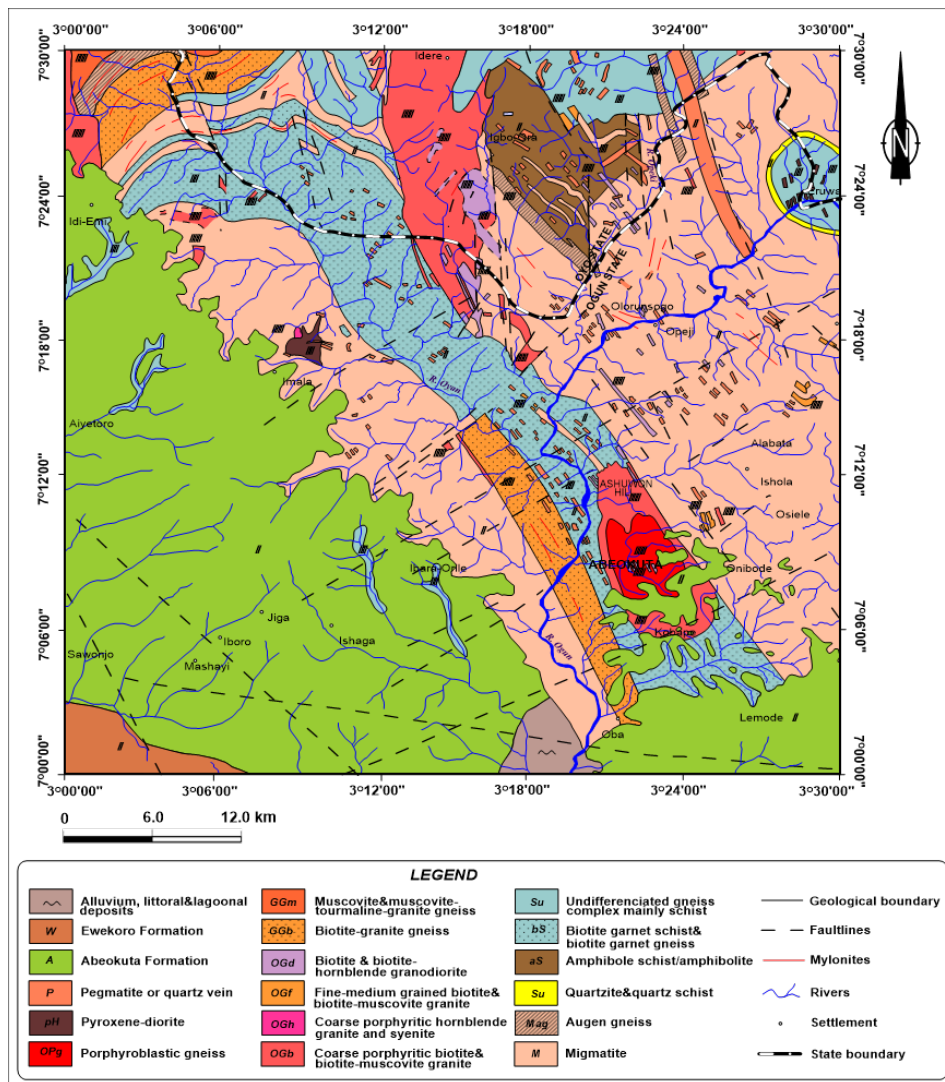


Figure 1. Geological Map of Abeokuta and its environs, a portion of eastern Dahomey Basin

The study area, presented as Figure 1, is found within latitudes 7° 00' N to 7° 30' N and longitudes 3° 00' E to 3° 30' E which corresponds to sheet no. 260 on the sheet index map of Nigeria. The portion in view covers an approximate area of about 3,025 square kilometers with an elevation range of 11 m to 256 m as described by the legend of ETOPO1 digital terrain model (DTM) represented as figure 2. Abeokuta and its environment share boundary with Oyo and Osun, Lagos, Ondo and Republic of Benin in the North, South, East and West respectively. According to [16], Abeokuta area is composed of magmatic older granites that are of Precambrian age to early Palaeozoic age. Rahaman posited that the gneiss-migmatite complex is more distributed over the Abeokuta area and comprises of quartzite, calcsilicate, gneisses, amphibolites and biotite-hornblende schist [17].

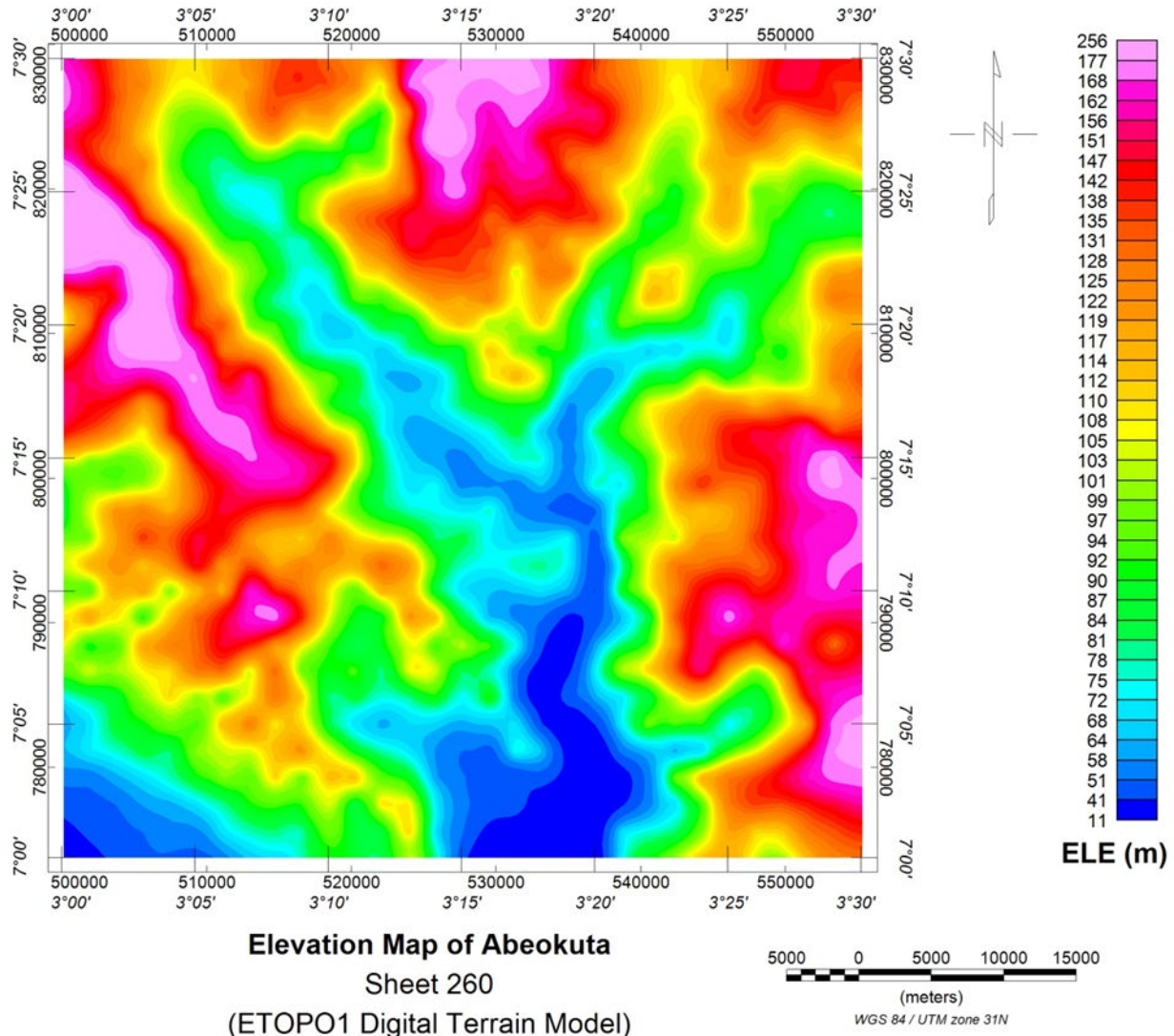


Figure 2. Elevation map of Abeokuta and its environs, generated from ETOPO1 map

2. Materials and methods

2.1. Data acquisition

The aeromagnetic data used in this research was obtained from the Nigeria Geological Survey Agency (NGSA). The NGSA employed the services of Fugro Airborne Surveys for the acquisition of the data. The acquisition of the dataset (sheet 260) was done between 2005 and

2007 with 3 x Scintrex CS3 Cesium vapour magnetometer using the FASDAS acquisition system. The data was acquired at a sensor mean terrain clearance of 80 m, flight line spacing of 500 m, tie line spacing of 5000 m, flight line trend of 135° and tie line trend of 45° [18]. The data recording interval was set at 0.1 s or less than 0.22 s, which is about 3 m to 7 m.

2.2. Data processing

According to Nigeria Geological Survey Agency [19], the dataset acquired was part-processed by Fugro Airborne Surveys using Universal Transverse Mercator of zone 32N (UTM-32N) projection and WGS 84 as the reference datum. De-culturing, tie line and micro-levelling are some of the pre-processing operations carried out on the data. The dataset was given out by NGSA as an ASCII file comprising of X, Y and Z columns corresponding to the longitudes, latitudes and their matching total magnetic field intensities respectively. The total magnetic field intensity 'Z' was stripped of 33,000 nT for ease of processing the airborne data [19].

The dataset was loaded in Oasis Montaj software database (Figure 3) to obtain the raw total magnetic field intensity (Z_Total) by addition of 33,000 nT earlier stripped off. The raw dataset was then re-projected to Universal Transverse Mercator of zone 31N (UTM-31N) in order to minimize distortions due to the curvature of the Earth and to have relationship with the subsurface geology for easier interpretations. This was necessary because the study location falls within UTM – 31N.

✓ D0:0	X	Y	Long UTM31N	Lat UTM31N	Long Deg	Lat Deg	TMI	Z Total	Dist	Inc	Dec	Out TotalF	TMA
6066.0	-112000	778700	551619.28	775110.01	3.28.02.48	7.00.43.49	59.85	33059.9	1201178.17	-11.4	-3.5	32639.2	420.6
6067.0	-111900	778700	551718.81	775111.29	3.28.05.73	7.00.43.53	59.84	33059.8	1201277.72	-11.4	-3.5	32639.3	420.5
6068.0	-111800	778700	551818.35	775112.57	3.28.08.97	7.00.43.57	59.85	33059.9	1201377.26	-11.4	-3.5	32639.4	420.4
6069.0	-111700	778700	551917.88	775113.84	3.28.12.22	7.00.43.60	59.89	33059.9	1201476.80	-11.4	-3.5	32639.5	420.4
6070.0	-111600	778700	552017.41	775115.12	3.28.15.46	7.00.43.64	59.94	33059.9	1201576.34	-11.4	-3.5	32639.6	420.3
6071.0	-111500	778700	552116.95	775116.39	3.28.18.71	7.00.43.68	59.98	33060.0	1201675.88	-11.4	-3.5	32639.7	420.3
6072.0	-111400	778700	552216.48	775117.67	3.28.21.95	7.00.43.72	60.01	33060.0	1201775.43	-11.4	-3.5	32639.8	420.2
6073.0	-111300	778700	552316.02	775118.95	3.28.25.19	7.00.43.76	60.00	33060.0	1201874.97	-11.4	-3.5	32639.9	420.1
6074.0	-111200	778700	552415.55	775120.22	3.28.28.44	7.00.43.80	59.98	33060.0	1201974.51	-11.4	-3.5	32640.0	420.0
6075.0	-111100	778700	552515.09	775121.50	3.28.31.68	7.00.43.83	59.95	33059.9	1202074.05	-11.4	-3.5	32640.1	419.9
6076.0	-111000	778700	552614.62	775122.77	3.28.34.93	7.00.43.87	59.91	33059.9	1202173.60	-11.4	-3.5	32640.2	419.7
6077.0	-110900	778700	552714.15	775124.05	3.28.38.17	7.00.43.91	59.88	33059.9	1202273.14	-11.4	-3.5	32640.3	419.6
6078.0	-110800	778700	552813.69	775125.33	3.28.41.42	7.00.43.95	59.87	33059.9	1202372.68	-11.4	-3.5	32640.4	419.5
6079.0	-110700	778700	552913.22	775126.60	3.28.44.66	7.00.43.99	59.88	33059.9	1202472.23	-11.4	-3.5	32640.5	419.4
6080.0	-110600	778700	553012.76	775127.88	3.28.47.90	7.00.44.03	59.94	33059.9	1202571.77	-11.4	-3.5	32640.6	419.4
6081.0	-110500	778700	553112.30	775129.16	3.28.51.15	7.00.44.06	60.01	33060.0	1202671.31	-11.4	-3.5	32640.7	419.4
6082.0	-110400	778700	553211.83	775130.43	3.28.54.39	7.00.44.10	60.00	33060.1	1202770.86	-11.4	-3.5	32640.7	419.3
6083.0	-110300	778700	553311.37	775131.71	3.28.57.64	7.00.44.14	60.12	33060.1	1202870.40	-11.4	-3.5	32640.8	419.3
6084.0	-110200	778700	553410.90	775132.98	3.29.00.88	7.00.44.18	60.14	33060.1	1202969.94	-11.4	-3.4	32640.9	419.2
6085.0	-110100	778700	553510.44	775134.26	3.29.04.12	7.00.44.22	60.16	33060.2	1203069.49	-11.4	-3.4	32641.0	419.1
6086.0	-110000	778700	553609.98	775135.54	3.29.07.37	7.00.44.25	60.23	33060.2	1203169.03	-11.4	-3.4	32641.1	419.1
6087.0	-109900	778700	553709.51	775136.81	3.29.10.61	7.00.44.29	60.35	33060.3	1203268.58	-11.4	-3.4	32641.2	419.1
6088.0	-109800	778700	553809.05	775138.09	3.29.13.86	7.00.44.33	60.48	33060.5	1203368.12	-11.4	-3.4	32641.3	419.2
6089.0	-109700	778700	553908.59	775139.37	3.29.17.10	7.00.44.37	60.60	33060.6	1203467.67	-11.4	-3.4	32641.4	419.2
6090.0	-109600	778700	554008.12	775140.64	3.29.20.35	7.00.44.41	60.67	33060.7	1203567.21	-11.4	-3.4	32641.5	419.2
6091.0	-109500	778700	554107.66	775141.92	3.29.23.59	7.00.44.45	60.71	33060.7	1203666.76	-11.4	-3.4	32641.6	419.1
6092.0	-109400	778700	554207.20	775143.19	3.29.26.83	7.00.44.48	60.75	33060.7	1203766.30	-11.4	-3.4	32641.7	419.0
6093.0	-109300	778700	554306.73	775144.47	3.29.30.08	7.00.44.52	60.80	33060.8	1203865.85	-11.4	-3.4	32641.8	419.0
6094.0	-109200	778700	554406.27	775145.75	3.29.33.32	7.00.44.56	60.85	33060.9	1203965.40	-11.4	-3.4	32641.9	419.0

Figure 3. Database for processing aeromagnetic dataset, sheet 26

2.3. Qualitative analysis

The Total Magnetic Intensity (TMI) map (Figure 4) and Raw Total Magnetic Field Intensity (RTMI, Figure 5) were produced by minimum curvature gridding algorithm as described by [20], using a grid cell size of 100 m. The International Geomagnetic Reference Field (IGRF) was calculated and removed from the RTMI (as illustrated by Figure 3, a database for processing the dataset) to obtain the actual Total Magnetic Anomaly (TMA), which represent the true intensity distribution of anomalies over the study location. A map of the TMA is presented as Figure 6.

2.3.1.Reduction to the magnetic equator (RTE)

Reduction to pole is the commonest filtering technique used in correcting for asymmetries of magnetic anomaly over sources [21-23]. Earth's field intensity decreases from the poles to the equator and as such the peaks of signals (magnetic anomalies) can possibly be wrongly centered over their sources, usually observed as abnormal alignment of signals in the E-W direction. However, at low latitudes, like this research area which is found around latitude 7°,

reduction to pole accentuate noises so much that the result of it is dominated by linear features aligned in the E-W direction. To correct for this kind of asymmetry for geologically meaningful interpretations, the Reduction to the Magnetic Equator filter (MAGMAP, a 2-D fast Fourier transform filter in Oasis Montaj Software) was applied on the TMA grid to centre the peak of signals over geologic sources. The Reduction to the Magnetic Equator (RTE) grid is represented by Figure 7 (RTE). The Radially Averaged Power Spectrum (Figure 8) was generated using the RTE grid to visualize deep seated and shallow magnetic sources as well as showing possible noise level.

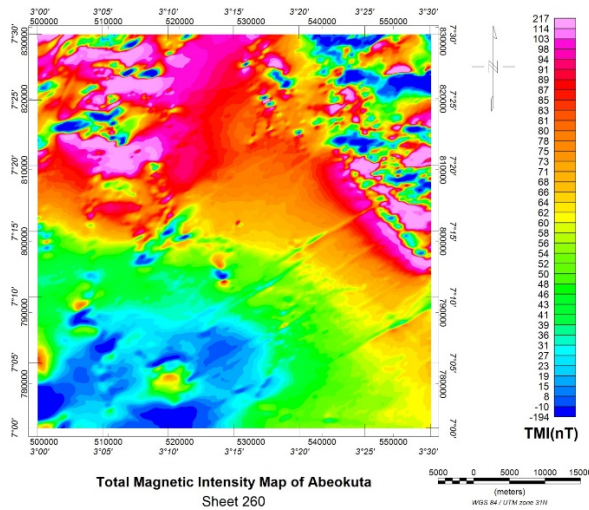


Figure 4. Total Magnetic Intensity (TMI) map, as supplied by NGSA

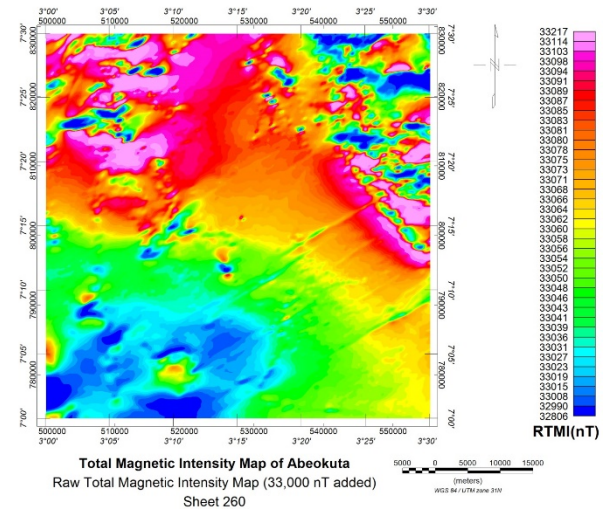


Figure 5. Raw Total Magnetic Intensity (RTMI) map (33,000 nT added to TMI)

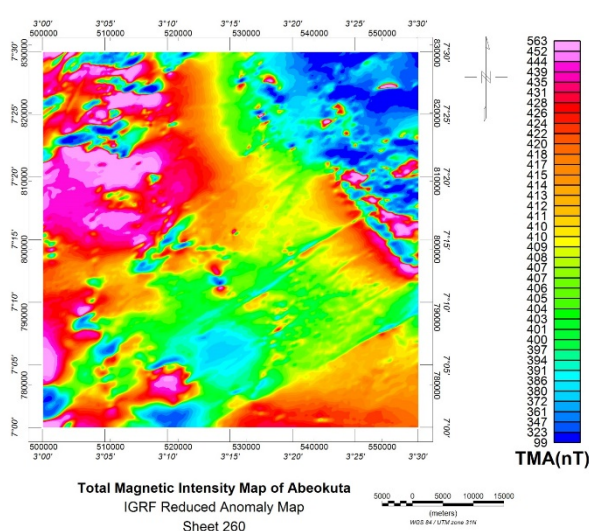


Figure 6. Total magnetic anomaly map

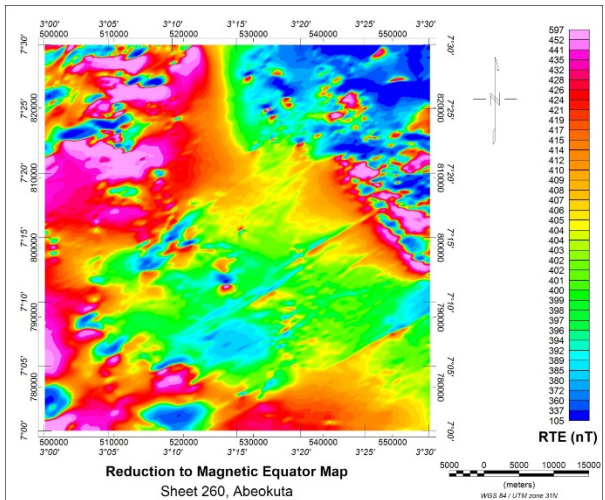


Figure 7. Reduction to magnetic equator map of Abeokuta and its environs

2.3.2. Derivatives filtering

Derivative filters play very important role in sharpening of anomalies' edges and enhancing subsurface features associated with shallow sources. A two dimensional fast Fourier transform (2-D FFT) filtering technique known as MAGMAP is a Geosoft executable incorporated into Oasis Montaj Software used in computing the different derivative grids by a step-by-step filtering processes. The derivative grids were produced to aid the interpretation of geologic boundaries and other linear features such as lineaments [24-25]. The directional derivative filter

was used in producing the horizontal derivative map of the study area along X (X-Der) direction presented as Figure 9 while the vertical derivative map (Z-Der, Figure 10) was estimated by defining the vertical derivative filter on the 2-D grid of RTE used in these computations.

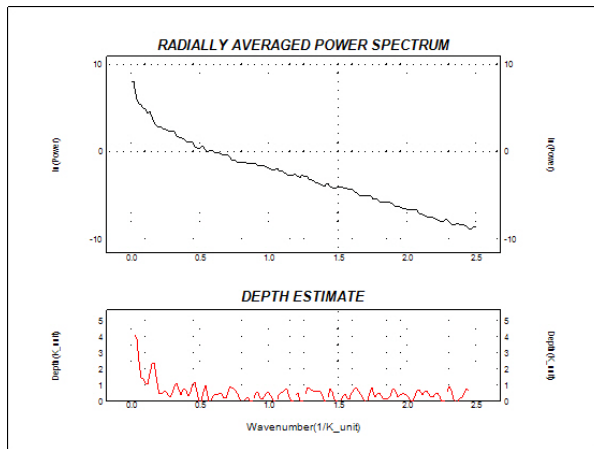


Figure 8. Radially averaged power spectrum

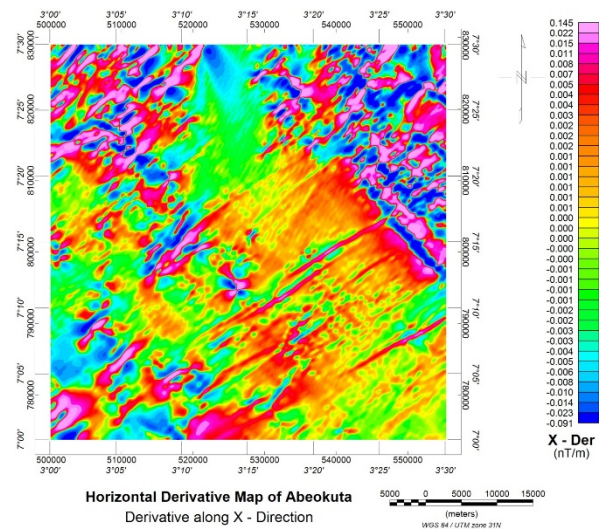


Figure 9. Horizontal derivative map of Abeokuta and its environs along the X-Direction

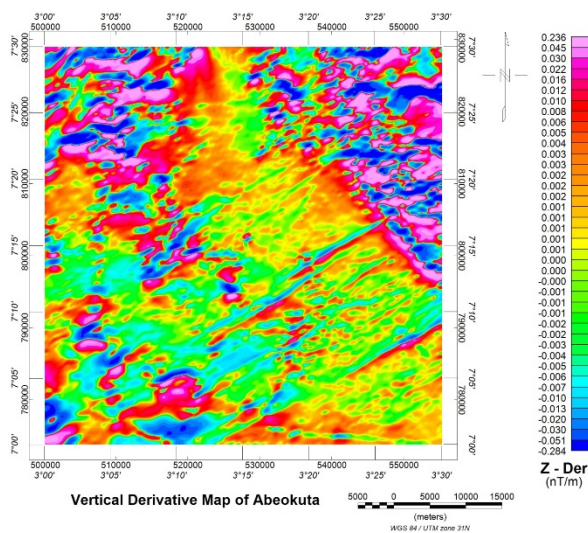


Figure 10. Vertical derivative map of Abeokuta and its environs

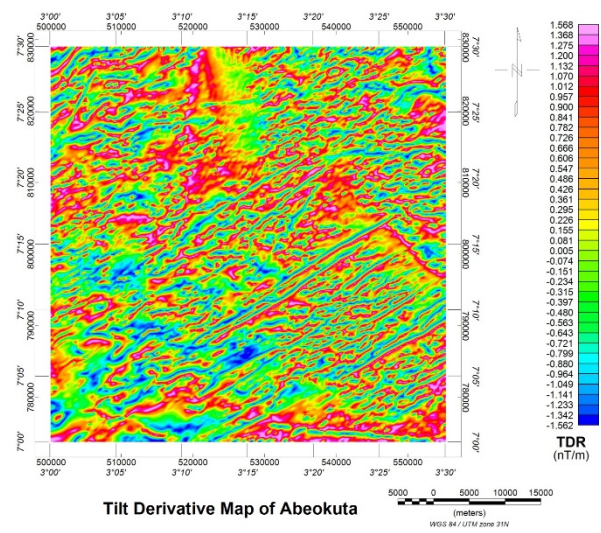


Figure 11. Tilt derivative map of Abeokuta and its environs

The horizontal derivative is expressed mathematically as:

$$F\left[\frac{d^n \phi}{dx, y^n}\right] = (ik_{x,y})^n F(\phi) \tag{1}$$

where: F = Fourier transform of the magnetic field; $n = 1, 2$; the n^{th} order horizontal derivative; ϕ = Potential of the field; $(ik_{x,y})$ is an operator which transform a function into n^{th} order derivative with respect to either x or y .

The first vertical derivative is expressed mathematically as:

$$F\left[\frac{d^n \phi}{dz^n}\right] = k^n F(\phi) \tag{2}$$

where: F = Fourier transform of the Magnetic field; $n = 1, 2$, the n^{th} order vertical derivative; ϕ = Potential of the field.

The Tilt derivative map (TDR) displayed as Figure 11 assumes that the source structures have vertical contacts and there is no remanent magnetization and the magnetization is vertical [26]. The Analytic Signal map (AS) displayed as Figures 12, showed the boundaries and edges of anomalies. Both maps were also produced by defining their filters through the step-by-step filtering techniques in MAGMAP.

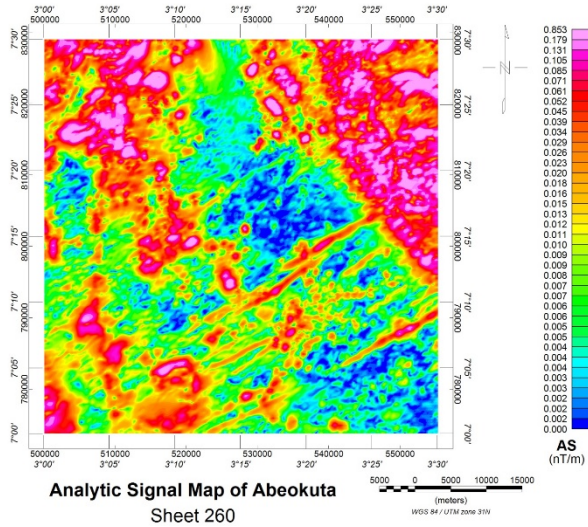


Figure 12. Analytic Signal Map of Abeokuta and its environs

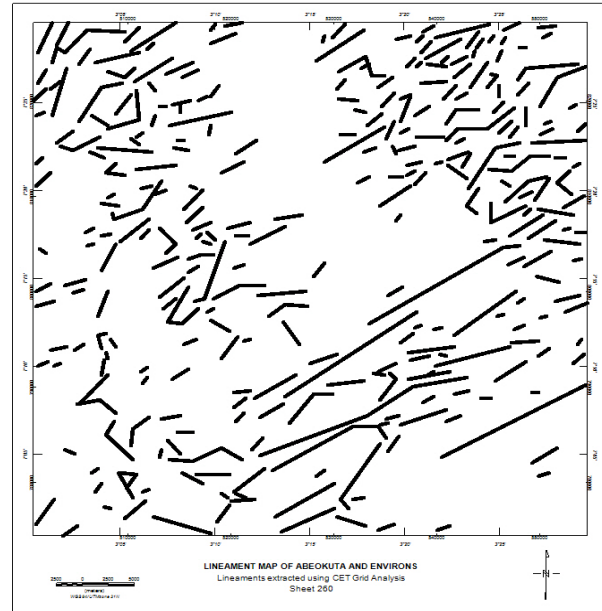


Figure 13. Extracted Lineament Map of Abeokuta and its environs

2.3.3. Lineament analysis

The Centre for Exploration Targeting (CET) grid analysis is another set of plugins (algorithms) used in the extraction of lineaments associated with the study area. It is developed by the Centre for Exploration Targeting, based at the University of Western Australia, which is incorporated into the Oasis Montaj Software as an executable. This computation and analysis is to identify areas of structural complexity through texture analysis, lineation detection, lineation vectorization and skeletonization, as well as thresholding. The Tilt derivative (Figure 11) grid was used as the mother grid for these computations and the extracted lineament map is presented as Figure 13.

These extracted lineaments were plotted as a Rose diagram, shown as Figure 14. The linear features are generally trending northeast of the study area; this trend is in agreement with the tectonic trend of Nigeria [27] and also in line with the evolutionary origin of Dahomey Basin according to [28].

2.4. Quantitative analysis

This approach involves making numerical estimates of certain magnetic signatures that yielded likely geological features and their depths of sources [3].

2.4.1. Source parameter imaging (SPI) method

The SPI is a depth estimation technique that uses an extension of complex analytic signal to estimate magnetic source depth according to [29]. It is a profile or grid based method developed by [30], which utilizes the relationship between the source depths and the local wave-number (K) of the observed field.

The analytic signal $A_1(x, z)$ is defined by [31] as:

$$A_1(x, z) = \frac{\partial M(x, z)}{\partial x} - j \frac{\partial M(x, z)}{\partial z} \quad (3)$$

where $M(x, z)$ is the magnitude of the anomalous total potential field, j is the imaginary number, and z and x are Cartesian coordinates for the vertical direction and the horizontal direction perpendicular to strike, respectively. [31] showed that the horizontal and vertical derivatives comprising the real and imaginary parts of the 2D analytical signal are related by

$$\frac{\partial M(x,z)}{\partial x} \Leftrightarrow -j \frac{\partial M(x,z)}{\partial z} \tag{4}$$

where \Leftrightarrow denotes a Hilberts transform pair.

The Local wavenumber K_1 is defined by [30] to be

$$K_1 = \frac{\partial}{\partial x} \tan^{-1} \left[\frac{\partial M}{\partial z} / \frac{\partial M}{\partial x} \right] \tag{5}$$

Thus, the analytic signal could be defined based on second-order derivatives, $A_2(x, z)$, where

$$A_2(x, z) = \frac{\partial^2 M(x,z)}{\partial z \partial x} - j \frac{\partial^2 M(x,z)}{\partial z^2} \tag{6}$$

This gives rise to a second-order local wave number K_2 , where

$$K_2 = \frac{\partial}{\partial x} \tan^{-1} \left[\frac{\partial^2 M}{\partial z^2} / \frac{\partial^2 M}{\partial z \partial x} \right] \tag{7}$$

The RTE grid (Figure 7) with its derivative components (X-Der, Y-Der, Z-Der and TDR) were used by this technique in the estimation of magnetic source depths and geometries. The result of this computation in a database was gridded to produce a 2D grid which represents the SPI map (Figure 15) with its sources depths.

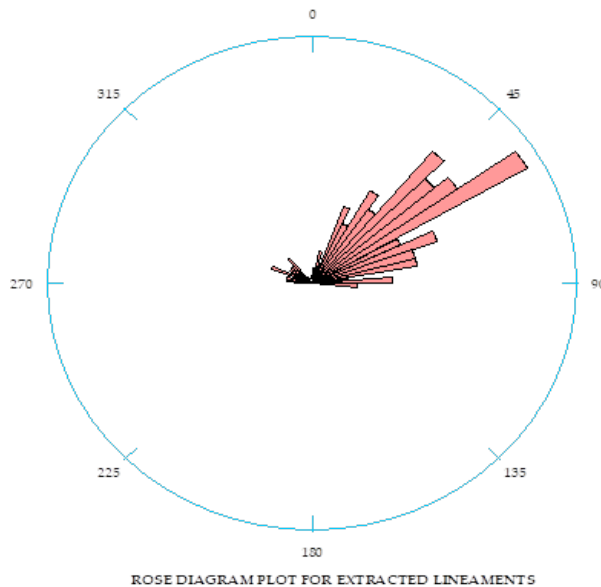


Figure 14. rose diagram plot for extracted lineament in the study area

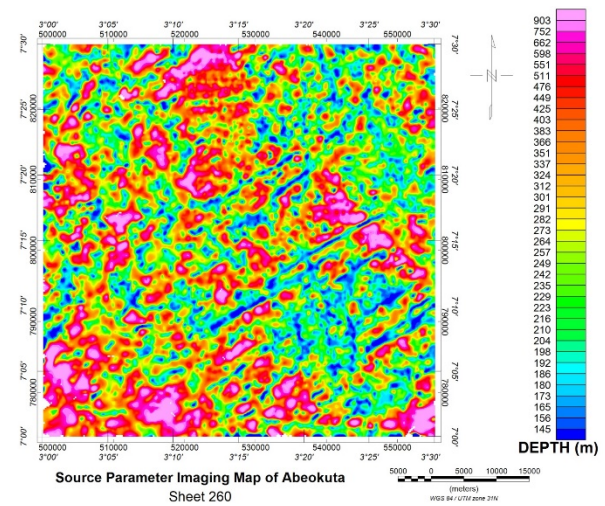


Figure 15. Source parameter imaging map of Abeokuta and its environs

2.4.2. 3-D Euler Deconvolution Method

Euler deconvolution is another depth evaluation technique, based on Hilbert’s transform and first applied to magnetic profile data by Thompson in 1982 [11] suggested approaches for the method’s application to a gridded data which was implemented by [32-34] further developed the method and generalized it to cope with a wider range of source types. The technique has been found more reliable by many researchers when compared with other depth techniques because of its specialty in producing suitable results even when the geological models are wrongly represented.

3-D Euler Deconvolution method is based on a system of linear equation called the ‘homogeneity equation’ which relates the potential field and its gradient components to the position of the source, with the degree of homogeneity η which is interpreted as a structural index, SI [11].

For the purpose of this research and with the pre-existing knowledge of the geology of the study area, parameters such as the grid interval, structural index, window size, maximum % depth tolerance and maximum distance were carefully chosen for this computation to obtain

the best results as suggested by [35]. The source geometry under investigation determines the structural index to be used [36]. SI = 0.0 for geologic contact, 1.0 for dyke of fault, 2.0 for vertical or horizontal cylinder and 3.0 for magnetic sphere. Table 1 shows the different source geometries with their corresponding structural indices.

The 3-D form of Euler’s equation can be defined mathematically as, [33, 37]:

$$x \frac{\partial T}{\partial x} + y \frac{\partial T}{\partial y} + z \frac{\partial T}{\partial z} + \eta T = x_0 \frac{\partial T}{\partial x} + y_0 \frac{\partial T}{\partial y} + z_0 \frac{\partial T}{\partial z} + \eta b \quad (8)$$

where: x, y and z are the coordinates of a measuring point; x₀, y₀ and z₀ are the coordinates of the source location whose total field is detected at x, y, and z; b is a base level; η is structural index (SI) and T is total potential field. Figures 16, 17 and 18 represent each of the structural index, SI = 0, 1 and 2 respectively.

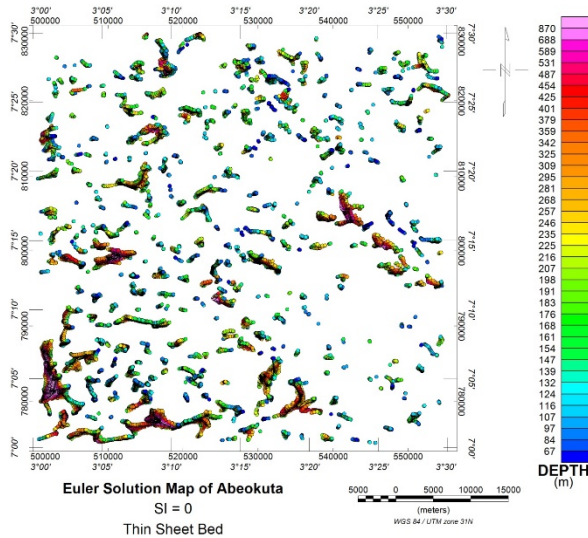


Figure 16. Euler solution map of Abeokuta and its environs, for SI = 0

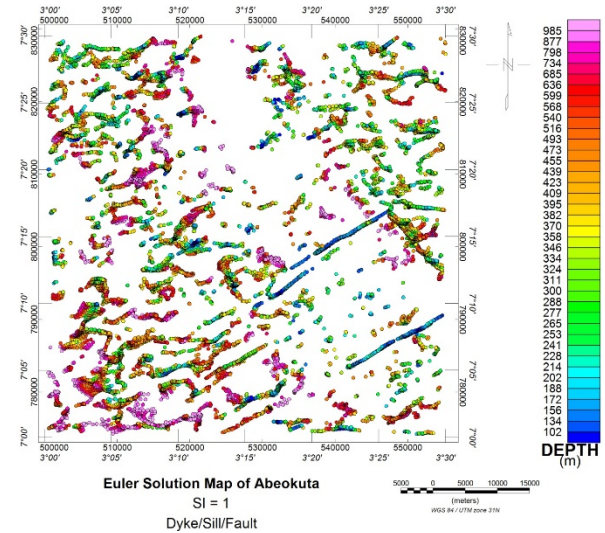


Figure 17. Euler solution map of Abeokuta and its environs, for SI = 1

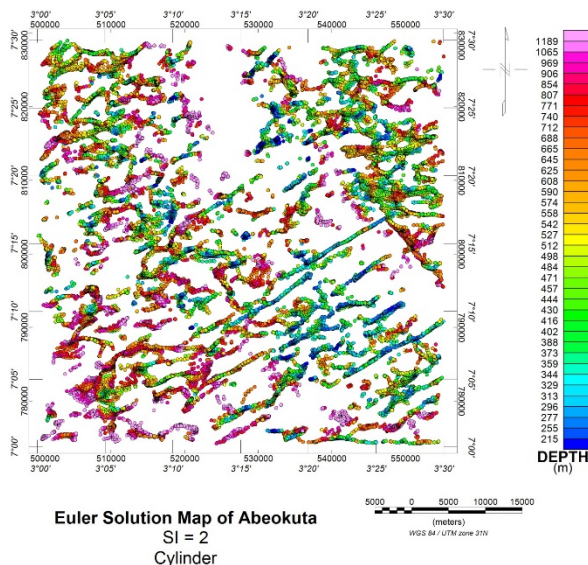


Figure 18. Euler solution map of Abeokuta and its environs, for SI = 2

Table 1. Structural index (SI) for magnetic sources of different source geometries

Source geometry	SI
Sphere	3
Vertical or horizontal line (cylinder)	2
Thin bed fault (Dyke)	1
Geologic contact	0

Source: Reid et al. [34]

3. Discussion and interpretation of results

Discussing the results is concerned with the geophysical interpretations of the results into more meaningful geological parameters defining the various findings of this research which include but not limited to the location and depth of magnetic sources.

3.1. Qualitative interpretation

The digitized dataset of Abeokuta and its environs (sheet 260) was presented as TMI (figure 4) and RTMI (Figure 5) after gridding. Both represent the total magnetic intensity map of the study location with three major distinctive magnetic intensities category of low, intermediate and high magnetic values. A magnetic amplitude range of 32,805 to 33217 nT was reflected from the legend of the figure. Low magnetic values of 32,805 to 33,018 nT observed around southern corner with splashes of its dots around the northwestern and northeastern regions. The intermediate magnetic intensities were found to be between 33,023 to 33,091 nT which are partly distributed all over the study area but majorly trending E-W direction while the high magnetic signatures correspond to values of 33,094 to 33,217 nT can be observed at the north, northeast and northwest of the maps. The differences in the lithological distributions are as a result of the different magnetic content (like sedimentary, metamorphic and igneous rock units) in the area. Abeokuta and its environs are predominantly covered with magnetic anomalies of intermediate intensities which possibly indicate the presence of magnetically susceptible minerals that are majorly Migmatite-Gneiss complex according to [14]. Anomalies with low magnetic responses observed at Sawonjo, Mashayi and Ibooro areas possibly predict the presence of some sedimentary rock units like shale and gypsum [38]. These observations conform to the geological realities in the research area in real sense.

The TMA (Figure 6) is a result of TMI reduced for IGRF, while the RTE represent the residual anomaly processed for quantitative analyses and interpretations. Low latitude effect cause magnetic signatures to be wrongly positioned over their sources and also make them skew along a particular direction [21-22], as seen as abnormal elongation of magnetic anomalies on the TMI map. The major fault lines are around SSE parts of the study area which have been made more conspicuous because anomalies have been rightly positioned over their sources by reducing the data to equator as observed on the RTE map (Figure 7).

The directional derivatives along X (X-Der), Y (Y-Der) directions and the vertical derivative (Z-Der) have ranges of -0.335 to 0.352 nT/m, -0.766 to 0.615 nT/m and -0.909 to 0.727 nT/m respectively. The tilt derivative map (TDR, figure 12) has its range to be -1.564 to 1.568 nT/m while the analytic signal (AS, figure 13) is from 0.000 to 917 nT/m. The derivatives have very similar and general trend of NE – SW. Regions of high concentration of magnetic bodies correspond to areas with high and positive values while zones of low magnetic bodies are having low values on the derivative maps. The AS has shown the edges of anomalies clearer and the TDR was used to extract lineaments by CET grid analysis through skeletonization, displayed as Figure 12. From the lineament map (Figure 14), the NE – SW trend is similar to the oceanic fractured zones that intruded into the study area from the Atlantic Ocean, these structural trends agree with Pan-African structural pattern [39]. The lineaments extracted can possibly serve as geologic contacts, faults and entrapments for the accumulation of mineralized targets.

3.2. Quantitative interpretation

Depth to basement evaluation of magnetic sources through SPI is displayed as Figure 16 and the legend of the figure reflects a minimum depth range of 145 to 180 m which represents the depths of shallow magnetic bodies. The maximum depth range as revealed by the SPI map is 598 to 903 m which corresponds to the depths of deeply seated magnetic anomalies. Patches of low and high magnetic anomalies can be observed to be intermingled in the study area due to the variations in magnetic susceptibilities of sources and undulations of the terrain. The linearly pronounced magnetic lows around the southeastern and central portions coincide

with the major faults of the area which are equally mapped in qualitative analysis. The sedimentary thickness (depth to basement) decreases from the south through to the north. Areas of high sedimentary thickness are the sedimentary terrain while areas of low sedimentary thickness are the basement complex of the study area.

Figures 17, 18 and 19 present the 3D Euler solution maps of different structural indices. Figure 1 is the result of Euler solution for the structural index of 1 which is used to solve for source geometry of a thin bed fault (Dyke/Sill/Fault). This solution is considered more appropriate because it contains less spurious solutions after windowing and geologically meaningful interpretations can be deduced from the map. A depth range of 102 to 985 m is seen on the figure. The figure displays a minimum depth range of 102 to 188 m which is considered to be the depth range of near surface intrusive rocks while the maximum depth range of 685 to 985 m depicts the location of long wavelength magnetic anomalies. The patterned continuous elongation of contours around the southeastern parts conforms to the fault structures interpreted in qualitative analysis and when compared with the geological map (Figure 1) of Abeokuta and environs. The blue/light blue colouration of the patterned contours interpreted as fault structures shows that they are found to be at shallow depths. Quantitative comparison of the SPI and 3D Euler Deconvolution reveal very close depth results.

4. Conclusion

The analyses of High Resolution Aeromagnetic Data of Abeokuta and its environs have helped to improve and deepen the knowledge of its geology. Qualitative analysis of the data aided the magnetic distributions of the study area. Low, moderate and high magnetic intensities are due to the likely presence of sedimentary, metamorphic and igneous rock units respectively. Steep gradient of contours observed by visualizing the maps are the possible fault lines in the study area, these fault lines are entrapments for the accumulation of mineral rocks. Quantitative analysis and interpretation of the data by the depth estimation techniques revealed a sedimentary thickness range of about 100 m to 1 km in the basement complex. 3D Euler Deconvolution method delineated the various geologic structures (such as faults, contacts, void, etc.) of the study area more conspicuously.

In general, the basement topography configured and other techniques used are guides to address various societal challenges. Areas identified as basement complex will be suitable for siting engineering constructions like railway, roads and other high-rise buildings while areas associated with fault lines should be avoided for these purposes because of the tendencies of early cracks.

Acknowledgement

The author acknowledged the individual contributions of the co-authors and particularly, the Nigeria Geological Survey Agency (NGSA) for making the data used for this research available.

Conflict of Interest

The authors have no contrasting interest, as to the production of this research.

References

- [1] Obiora DN, Dimgba BC, Oha IA, and Ibuot JC. Airborne and Satellite Geophysical Data Interpretation of the Gubio Area in the Bornu Basin, Northeastern Nigeria: Implication for Hydrocarbon Prospectivity. *Pet Coal*, 2020; 62(4), 1504-1516.
- [2] Ofoha CC, Emujakporue G, and Ekine AS. Interpretation of Aeromagnetic Anomalies of Degema and Oloibiri area of Niger Delta Nigeria using Qualitative Approach. *Journal of Scientific Research & Reports*, 2018; 18(4): 1-12.
- [3] Revees C. *Aeromagnetic Surveys; Principles, Practice and Interpretation*. GEOSOFT, 2005; 155.
- [4] Nabighian MN, Hansen RO. Unification of Euler and Werner deconvolution in three dimensions via the generalized Hilbert transform. *Geophysics*, 2005; 66.
- [5] Osinowo OO, and Olayinka AI. Aeromagnetic Mapping of Basement Topography around the Ijebu-Ode Geological Transition Zone, Southwestern Nigeria. *Acta Geod Geophysics*, 2013; 13(48): 451-470.

- [6] Layade GO, Edunjob, HO, Makinde V, and Bada BS. Application of Forward and Inverse Modelling to High-Resolution Data for Mineral Exploration. *International Journal of Earth and Space Physics*, 2021; 46(4): 117-129.
- [7] Akinse AG, and Gbadebo AM. Geological mapping of Abeokuta Metropolis, Southwestern Nigeria. *International Journal of Scientific & Engineering Research*, 2016;7(8): 979-983.
- [8] Bello R, and Falano OC. Interpretation of Aeromagnetic Anomalies over Abeokuta, Southwest Nigeria, using Spectral Depth Technique. *Journal of Applied Sciences in Environmental Management*, 2017; 21(2): 218-222.
- [9] Olurin OT, Olowofela JA, Akinyemi OD, Badmus BS, Idowu OA, and Ganiyu SA. Enhancement and Basement Depth Estimation from Airborne Magnetic Data. *African Review of Physics*, 2015; 10(38): 303-313.
- [10] Olowofela JA, Akinyemi OD, Badmus BS, Awoyemi MO, Olurin,OT, and Ganiyu SA. (2013), Depth estimation and source location of Magnetic anomalies from a Basement Complex Formation, using Local Wavenumber Method (LWM). *IOSR Journal of Applied Physics*, 2013; 4(2): 33-38.
- [11] Thompson DT. A new technique for making computer-assisted depth estimates from magnetic data. *Geophysics*, 1982; 47(1): 31-37.
- [12] Okpoli CC, and Eyitoyo FB. Aeromagnetic Study of Okitipupa Region, Southwestern Nigeria. *International Basic and Applied Research Journal*. 2016; 2(7): 1-20.
- [13] Osinowo OO, Adebajji MA, and Adewoye OA. Structural Interpretation and Depth Estimation from Aeromagnetic Data of Abigi-Ijebu Waterside area of Eastern Dahomey Basin, Southwestern Nigeria. *Geofisica Internacional.*,2019; 58(4): 259-277.
- [14] Obaje NG. Geology and mineral resources of Nigeria. *Lecture Note in Earth Science*, 2009
- [15] Oli IC, Okeke OC, Abiahu CMG, Anifowose FA, and Fagorite VI. Review of the Geology and Mineral Resources of Dahomey Basin, Southwestern Nigeria. *International Journal of Environmental Sciences and Natural Resources*, 2019; 21(1): 36-40.
- [16] Jones HA and Hockey RO. The Geology of Parts of Southwestern Nigeria. *Bull. Geological Survey Nigeria*, 1964; 31: 101 – 102.
- [17] Rahaman OJ. Review of Basement Geology of Smith, Western Nigeria 1976.
- [18] NGSA (2005), Nigeria Geological Survey Agency (NGSA). Airborne Geophysical Digital Data Dissemination Guideline.
- [19] NGSA (2017), Nigeria Geological Survey Agency (NGSA). High Resolution Airborne Geophysical Survey.
- [20] Webring M. MINC. A Gridding Programme based on Minimum Curvature. *U.S Geological Survey Open-File Report.*, 1981; 81-1224, 43p.
- [21] Baranov V, and Naudy H. Numerical Calculation Of The Formula Of Reduction To The Magnetic Pole. *Geophysics*, 1964; 29: 67–79.
- [22] Keating P, and Zerbo L. An Improved Technique for Reduction to the Pole at Low Latitudes. *Geophysics*, 1996; 61(1), 131-137.
- [23] Salem A, Williams S, Fairhead JD, Ravat D, and Smith R. Tilt Depth Method: A Simple Depth Estimation Method Using First-Order Magnetic Derivatives: The Leading Edge, 2007; 26, 1502–1505
- [24] Ferreira FJF, de Castro LG, Bongioiolo ABS, de Souza J, and Romeiro MAT. Enhancement of the Total Horizontal Gradient of Magnetic Anomalies using Tilt Derivatives: Part II—Application to real data: 81st Annual International Meeting, SEG, Expanded Abstracts, 2011; 887–891.
- [25] Verduzco B, Fairhead JD, and Green CM. New Insights into Magnetic Derivatives for Structural Mapping. *The Leading Edge*, 2004; 23 (2): 116–119.
- [26] Rasak B, Musa H, Basseyy NE and Usman K. Depth Estimation, Structural Features and Mineralization from High Resolution Aeromagnetic and Satellite Data over Yola Arm of the Upper Benue and Adjoining Basement Regions, Northeastern Nigeria. *Pet Coal*, 2020; 62(4), 1163-1171.
- [27] Dike EFC. Sedimentation and tectonic evolution of the upper Benue trough and Bornu Basin, ND Nigeria (Abstract), in: Nigerian Mining and Geosciences Society annual international conference, Port Harcourt, Nigeria, March 4 – 8th, 2002.
- [28] Gulraud M. Tectono-Sedimentary framework of the early cretaceous continental Bima Formation (upper Benue trough, NE Nigeria). *Journal of African Earth Sciences*, 1990; (10): 341-353.
- [29] Nwosu OB. Determination of Magnetic Basement Depth over Parts of Middle Benue Trough By Source Parameter Imaging (SPI) Technique Using HRAM. *International Journal of Scientific and Technology Research*, 2014; 3(1): 262-271.

- [30] Thurston JB, and Smith RS. Automatic conversion of magnetic data to depth, dip and density contrast using the SPI™ method. *Geophysics*, 1997; 62 (3): 807-813.
- [31] Nabighian MN. The analytic signal of 2-D magnetic bodies with polygonal cross sections; its properties and use for automated anomaly interpretation. *Geophysics*, 1972; 37, 507-517.
- [32] Mushayandebvu MF, van Drie, P, Reid AB, and Fairhead JD. Magnetic source parameters of two-dimensional structures using extended Euler deconvolution. *Geophysics*, 2001; 66: 814-823.
- [33] Reid AB, Allsop JM, Granser H, Millett AJ, and Somerton IW. Magnetic Interpretation in Three Dimensions using Euler Deconvolution. *Geophysics*, 1990; 55: 80-99.
- [34] Ravat D. (2007). Reduction to Pole. *Encyclopedia of Geomagnetism and Paleomagnetism*, D. Gubbins and E. Herrero-Bervera (eds.), Springer, 856–857.
- [35] Reid AB, Allsop JM, and Thurston JB. The structural index in gravity and magnetic Interpretation: Errors, uses and abuses. *Geophysics*, 2014; 79(4): 61-66.
- [36] Whitehead N, and Musselman C. MontajGrav/Mag interpretation: Processing, analysis and visualization system for 3D inversion of potential field data for Oasis montaj v6.1. Geosoft Inc. ON, Canada 2005.
- [37] Adegoke JA, and Layade GO. (2019): Comparative depth estimation of iron-ore deposit using the Data-Coordinate Interpolation Technique for airborne and ground magnetic survey variation. *African Journal of Science, Technology, Innovation and Development*, 2019; 11(5): 663-669.
- [38] Telford WM, Geldart LP, and Sheriff RE. *Applied geophysics* (2nd edition), Cambridge University Press 1990, Cambridge.
- [39] Kaki C, d'Almeida GAF, Yalo N and Amelina S. Geology and Petroleum Systems of the Offshore Benin Basin (Benin). *Oil & Gas Science and Technology - Rev. IFP Energies nouvelles*, 2013; 68(2): 363-381

To whom correspondence should be addressed: Hazeez Owolabi Edunjobi, Department of Physics, Federal University of Agriculture, Abeokuta, Nigeria, E-mail: edunjobihazeez@gmail.com